JVI Journals.ASM.org

An ITAM in a Nonenveloped Virus Regulates Activation of NF-κB, Induction of Beta Interferon, and Viral Spread

Rachael E. Stebbing,[a] Susan C. Irvin,[a]* Efraín E. Rivera-Serrano,[a] Karl W. Boehme,[b,c]* Mine Ikizler,[b,c] Jeffrey A. Yoder,[a] Terence S. Dermody,[b,c,d] Barbara Sherry[a]

Department of Molecular Biomedical Sciences and Center for Comparative Medicine and Translational Research, North Carolina State University, Raleigh, North Carolina, USA[a]; Department of Pediatrics,[b] Elizabeth B. Lamb Center for Pediatric Research,[c] and Department of Pathology, Microbiology, and Immunology,[d] Vanderbilt University School of Medicine, Nashville, Tennessee, USA

Immunoreceptor tyrosine-based activation motifs (ITAMs) are signaling domains located within the cytoplasmic tails of many transmembrane receptors and associated adaptor proteins that mediate immune cell activation. ITAMs also have been identified in the cytoplasmic tails of some enveloped virus glycoproteins. Here, we identified ITAM sequences in three mammalian reovirus proteins: μ2, σ2, and λ2. We demonstrate for the first time that μ2 is phosphorylated, contains a functional ITAM, and activates NF-κB. Specifically, μ2 and μNS recruit the ITAM-signaling intermediate Syk to cytoplasmic viral factories and this recruitment requires the μ2 ITAM. Moreover, both the μ2 ITAM and Syk are required for maximal μ2 activation of NF-κB. A mutant virus lacking the μ2 ITAM activates NF-κB less efficiently and induces lower levels of the downstream antiviral cytokine beta interferon (IFN-β) than does wild-type virus despite similar replication. Notably, the consequences of these μ2 ITAM effects are cell type specific. In fibroblasts where NF-κB is required for reovirus-induced apoptosis, the μ2 ITAM is advantageous for viral spread and enhances viral fitness. Conversely, in cardiac myocytes where the IFN response is critical for antiviral protection and NF-κB is not required for apoptosis, the μ2 ITAM stimulates cellular defense mechanisms and diminishes viral fitness. Together, these results suggest that the cell type-specific effect of the μ2 ITAM on viral spread reflects the cell type-specific effects of NF-κB and IFN-β. This first demonstration of a functional ITAM in a nonenveloped virus presents a new mechanism for viral ITAM-mediated signaling with likely organ-specific consequences in the host.

Immunoreceptor tyrosine-based activation motifs (ITAMs) consist of YxxI/Lx$_{(6-12)}$YxxI/L sequences and are present in the cytoplasmic tails of certain transmembrane proteins, particularly those associated with immune cell activation. Examples include B-cell and T-cell receptors, as well as receptor-associated adaptor proteins such as DAP12 (1). Upon ligand-receptor binding, the ITAM-containing protein recruits Src family kinases for phosphorylation of the two conserved ITAM tyrosine residues (1, 2). Phosphorylated ITAMs then recruit Syk family kinases through interactions with Syk SH2 domains, inducing Syk autophosphorylation and subsequent downstream signaling (3, 4). Cellular ITAMs signal through intermediates, including mitogen-activated protein kinases (MAPKs), NFAT, and NF-κB, to stimulate an array of responses, such as cellular differentiation, cytokine release, and cell death (1, 3, 5–7).

ITAMs also have been identified in enveloped viruses, where they utilize the same signaling intermediates as cellular ITAMs and function in pathogenesis and oncogenesis (8). For example, hantavirus strains that cause hantavirus pulmonary syndrome contain an ITAM in the cytoplasmic tail of the G1 envelope protein, while nonpathogenic hantavirus strains lack this motif (9). Similarly, an ITAM in the Nef protein of simian immunodeficiency virus (SIV) is an important virulence determinant (10). All other known viral ITAMs are associated with oncogenic viruses in the *Herpesviridae* (11, 12) and *Retroviridae* (11, 13) families. To date, an ITAM-like sequence has been identified in only one nonenveloped virus, coxsackievirus; however, evidence for ITAM function in that virus remains ambiguous (14).

Mammalian orthoreoviruses (reoviruses), members of the *Reoviridae* family, are nonenveloped double-stranded RNA viruses that exhibit strain-specific differences in tropism and virulence in newborn mice (15). Reoviruses cause a spectrum of disease in these animals, including myocarditis, encephalitis, hepatitis, and hydrocephalus (15). Reovirus strain-specific differences in the capacity to induce myocarditis (cardiac tissue damage and inflammation) in mice correlate with virus strain-specific differences in induction of and sensitivity to the antiviral cytokine, beta interferon (IFN-β), in cardiac myocytes (16). Concordantly, nonmyocarditic reovirus strains induce cardiac lesions when the IFN response is disrupted (16–18). The reovirus M1 gene is the primary determinant of reovirus myocarditic potential (19, 20). The M1 gene encodes the μ2 protein, which is a minor constituent of the virion core but is abundant in the viral factories (VFs) that represent cytoplasmic sites of viral replication (15). Differences in the induction of and sensitivity to IFN-β segregate primarily with the reovirus M1 gene, as well as with the S2 and L2 genes, which encode the σ2 and λ2 proteins, respectively (16). While the M1 genes of reovirus strains that display resistance to IFN-β encode a

Received 4 September 2013 **Accepted** 9 December 2013
Published ahead of print 18 December 2013
Editor: D. S. Lyles
Address correspondence to Barbara Sherry, barbara_sherry@ncsu.edu.
R.E.S. and S.C.I. contributed equally to this article.
* Present address: Susan C. Irvin, Albert Einstein College of Medicine, Bronx, New York, USA; Karl W. Boehme, University of Arkansas for Medical Sciences, Little Rock, Arkansas, USA.

doi:10.1128/JVI.02573-13

repressor of IFN signaling (21), other reovirus effectors that modulate the IFN response are unclear.

Reoviruses induce IFN by activating pathogen recognition receptors RIG-I or MDA5 (17, 22, 23). Viral RNA synthesis occurs within the infecting particle and newly formed cores from which nascent single-stranded RNA is extruded (15). However, the reovirus RNA species that triggers RIG-I or MDA5 is undefined. IFN transcription factors IRF3 and NF-κB are activated upon reovirus infection, and activation of IRF3 is dependent on RIG-I and the adaptor protein MAVS (IPS-1). However, activation of NF-κB requires neither of these signaling intermediaries (17). The activation of NF-κB during reovirus infection also plays a role in apoptosis, which is cell type specific (18). Importantly, apoptosis induced by reovirus requires NF-κB in many cell types (24, 25) but not in cardiac myocytes (18, 26).

In this study, we identified ITAM sequences in the reovirus σ2, μ2, and λ2 proteins. We found that the μ2 ITAM in reovirus strain type 3 Dearing (T3D) is functional, recruiting the ITAM signaling intermediate Syk to VFs for activation of NF-κB and induction of IFN-β. In L929 cells, where NF-κB is required for reovirus-induced apoptosis, the μ2 ITAM enhances viral fitness. In contrast, in primary cardiac myocyte cultures where the IFN response is critical for antiviral protection and NF-κB is not required for apoptosis (18, 26), the μ2 ITAM limits viral fitness. These results suggest that the μ2 ITAM has a cell type-specific function in viral spread, likely reflecting the cell type-specific functions of NF-κB and IFN-β, and provide evidence of a new mechanism for ITAM-mediated signaling by a nonenveloped virus.

MATERIALS AND METHODS

Cell lines. Mouse L929 cells were maintained in minimal essential medium (MEM; SAFC Biosciences) supplemented to contain 5% fetal calf serum (FCS) (Atlanta Biologicals) and 2 mM L-glutamine (Mediatech). L929 cells were plated at 1.25×10^4 or 5×10^5 cells per well in 96-well or 24-well clusters, respectively, and incubated 3 h (h) prior to infection or transfection. HEK-293 cells (American Type Culture Collection [ATCC], CRL-1573) and AD-293 cells (Agilent Technologies), a derivative of HEK-293 cells with improved adherence, were maintained in Dulbecco MEM (DMEM; Gibco) supplemented to contain 10% FCS and 110 mg of sodium pyruvate (Mediatech)/liter. HEK-293 cells were plated at 3.5×10^4 cells or 4×10^5 cells per well in 96-well or six-well clusters, respectively. AD-293 cells were plated at 1.875×10^4 or 4×10^5 cells per well in 96-well or six-well clusters, respectively. HEK-293 and AD-293 cells were incubated at least 3 h prior to transfection or overnight before infection. Vero cells (ATCC, CCL-81) were maintained in DMEM supplemented to contain 10% FCS and were plated at 5×10^4 cells per well in 8-well collagen-coated chamber slides (BD BioSciences) 1 day prior to transfection.

Primary cardiac myocyte cultures. Timed-pregnant Cr:NIH(S) mice from the National Cancer Institute were maintained as a colony in a facility accredited by the Association for Assessment and Accreditation of Laboratory Animal Care. All animal procedures were approved by the North Carolina State University Institutional Animal Care and Use Committee. Primary cardiac myocyte cultures were generated from 1-day-old neonatal or term fetal Cr:NIH(S) mice resulting from timed pregnancies. Neonatal or term fetal mice were euthanized, and hearts were removed and treated with trypsin (27). To separate cardiac myocytes from rapidly adherent cardiac fibroblasts, cells were plated at 1.25×10^5 cells per well in six-well clusters and incubated for 2 h at 37°C. Cardiac myocytes were resuspended in DMEM supplemented to contain 7% FCS (Atlanta Biologicals), 0.06% thymidine (Sigma-Aldrich), and 10 μg of gentamicin (Sigma-Aldrich)/ml. Myocyte cultures contained ≤5% contamination with fibroblasts and were never passaged prior to use (21). Myocyte cultures were plated at 1.5×10^5 or 5×10^5 cells per well in 96-well or 48-well clusters, respectively, and incubated for 2 days prior to infection.

Viruses. Wild-type (WT) reovirus strain T3D and mutant recombinant viruses were generated using plasmid-based reverse genetics (28). Tyrosine-to-phenylalanine mutations in the ITAMs were introduced into plasmids containing the T3D S2, M1, or L2 genes (28, 29) using a QuikChange site-directed mutagenesis kit (Agilent Technologies) according to the manufacturer's instructions with the following primers: σ2 Y130F, forward (5′-GTACGACTGCGATGATTTTCCATTTCTAGCGC GTG-3′) and reverse (5′-CACGCGCTAGAAATGGAAAATCATCGCAG TCGTAC-3′); σ2 Y144F, forward (5′-GATTCAAACATCGGGTGTTTC AGCAATTGAGTGCTGTAAC-3′) and reverse (5′-GTTACAGCACTCA ATTGCTGAAACACCCGATGTTTGAATC-3′); μ2 Y118F, forward (5′-CTCAGGAAAGATGATGAATTCAATCAGCTAGCGCGTGC-3′) and reverse (5′-GCACGCGCTAGCTGATTGAATTCATCATCTTTCCTGA G-3′); μ2 Y131F, forward (5′-CAAGATATCGGATGTCTTCGCACCT CTCATCTCATCC-3′) and reverse (5′-GGATGAGATGAGAGGTGC GAAGACATCCGATATCTTG-3′); λ2 Y671F, forward (5′-CTTGGAC ATCTGGAGTGTTCTTCTTCTTGGTGGACC-3′) and reverse (5′-G GTCCACCAAGAAGAAGAACACTCCAGATGTCCAAG-3′); and λ2 Y681F, forward (5′-GGTGGACCATTTTTATCGTTTTGAGACTTTA TCTACGATCTCACG-3′) and reverse (5′-CGTGAGATCGTAGATA AAGTCTCAAAACGATAAAAATGGTC CACC-3′). Monolayers of BHK-T7 cells at 90% confluence (3×10^6 cells) seeded in 60-mm dishes were cotransfected with plasmids representing the cloned reovirus genome using 3 μl of TransIT-LT1 transfection reagent (Mirus) per μg of plasmid DNA (30). After 1 to 5 days of incubation, recombinant virus was isolated from transfected cells by plaque purification using monolayers of L929 cells. To confirm sequences of the mutant viruses, viral RNA was extracted from purified virions, subjected to One-Step reverse transcription-PCR (RT-PCR; Qiagen) using gene-specific primers, and sequenced. Recombinant viruses were plaque purified, amplified using L929 cells, purified using CsCl-gradient centrifugation, and stored as diluted aliquots at −80°C (31).

Plasmids. The luciferase reporter plasmid pNF-κB-luc and internal control reporter plasmid pRenilla-luc were previously described (32). The reporter plasmid pISRE-luc (Stratagene) encodes five tandem copies of the ISG54 interferon-stimulated response element (ISRE) 5′ to a gene encoding firefly luciferase. The reporter plasmid pIFN-β-luc was provided by John Hiscott (McGill University, Montreal, Canada). An effector plasmid expressing T3D μ2 in a pCAGGs backbone (pCAGGS-μ2) was generated previously (29). To generate the pFLAG plasmid, a FLAG tag was inserted between the NotI and XbaI restriction sites of pcDNA3 (Invitrogen) using the forward and reverse primers 5′-GGCCGCGATTACA AGGATGACGACGATAAGTAAT-3′ and 5′-CTAGATTACTTATCGTC GTCATCCTTGTAATCGC-3′, respectively. To generate pFLAG-μ2, the T3D M1 gene was subcloned into the EcoRI and NotI restriction sites of pFLAG using a primer that removed the μ2 stop codon and inserted one extra nucleotide to maintain the FLAG tag in-frame at the C terminus of μ2. To generate pFLAG-μ2-YYFF, both tyrosine residues in the ITAM were substituted with phenylalanine using a QuikChange site-directed mutagenesis kit. To maximize μ2 and μ2-YYFF expression (see Fig. 2, 4, and 5), the upstream Kozak sequence was optimized by changing ACC ATGG to GCCACCATGG. The plasmid pFLAG-NS3/4A expresses FLAG-tagged NS3/4A from hepatitis C virus in a pcDNA backbone. A plasmid expressing human Syk in a pcDNA3 backbone was provided by Sheng Wei (H. Lee Moffitt Cancer Center and Research Institute, Tampa, FL). A plasmid expressing green fluorescent protein (GFP)-tagged T1L μNS in a pEGFP-N1 backbone was provided by John Parker (Cornell University, Ithaca, NY). A plasmid expressing hemagglutinin (HA)-tagged T1L μ2 was generated from pCAGGS-M1-T1L (29) using the primer 5′-CCCGGGTCAGCTAGCGTAATCTGGAACATCGTATGGG TACGCCAAGTCAGATCGGAAAGCTAGTC-3′.

Transfections. For all comparisons within an experiment, the total DNA and FuGene concentrations were held constant by including addi-

tional vector DNA. For Fig. 2, each well of a six-well cluster of AD-293 cells was transfected with a 100-μl reaction mixture containing 3 μl of FuGENE 6 (Promega) and 1 μg of effector plasmid. For Fig. 3, each well of a 96-well or 6-well cluster of HEK-293 cells was transfected with 5 μl or 100 μl of 100-μl reaction mixtures containing 6 μl of FuGENE 6, 0.1 μg of pRenilla-luc, 1 μg of reporter plasmid, and 1, 0.1, or 0.05 μg of effector plasmid. For Fig. 4, Syk was inhibited by incubating AD-293 cells in 96-well or 6-well clusters with 25 mM piceatannol (EMD Calbiochem) dissolved in dimethyl sulfoxide (DMSO; Sigma-Aldrich) or DMSO alone as a control (final 1% DMSO). After 1 h, AD-293 cells were transfected using 10 μl (96-well) or 100 μl (6-well) of a 200-μl reaction. For 96-well clusters, each 200-μl reaction mixture contained 3 μl of Lipofectamine 2000 (Life Technologies), 0.1 μg of pRenilla-luc, 1 μg of reporter plasmid, and 0.1 μg of effector plasmid. For 6-well clusters, each 200-μl reaction mixture contained 3 μl of Lipofectamine 2000, 1 μg of pRenilla-luc, and 1 μg of effector plasmid. For Fig. 5, Vero cells were plated on 8-well chamber slides and transfected with 60 μl of a 100-μl reaction mixture containing 3 μl of FuGENE 6, 0.025 μg of Syk plasmid, 1 μg of μNS plasmid, and 1 μg of effector plasmid. For Fig. 6A, each well of a 96-well cluster of AD-293 cells was transfected with 5 μl of a 100-μl reaction mixture contained 3 μl of FuGENE 6, 0.1 μg of pRenilla-luc, and 1 μg of pNF-κB-luc. At 24 h posttransfection, AD-293 cells were washed twice with media, infected, incubated at 37°C for 1 h, supplemented with media, and incubated as indicated.

Luciferase assay. Transfected cells in 96-well clusters were lysed, and the luciferase activity was quantified by using a dual luciferase reporter assay system (Promega) according to the manufacturer's instructions. The luciferase activity for each sample was normalized to the internal *Renilla* luciferase control.

Antibodies for immunoblot analysis. Antibodies were used at the indicated final dilutions: mouse monoclonal anti-FLAG M2 (1:1,000; Agilent Technologies, catalog no. 200472-21) (Fig. 2), mouse monoclonal anti-FLAG M2 (1:2,500; Sigma-Aldrich, catalog no. F3165) (Fig. 3), rabbit polyclonal anti-μ2 (1:500; generated against two μ2 peptides by Open Biosystems), mouse monoclonal anti-phosphotyrosine 4G10 (1:1000; Millipore, catalog no. 05-321), goat polyclonal horseradish peroxidase (HRP)-conjugated anti-GAPDH (1:160; Santa Cruz Biotechnology, no. sc-20357-HRP), goat polyclonal HRP-conjugated anti-actin (1:500; Santa Cruz Biotechnology, catalog no. sc-1615), polyclonal HRP-conjugated goat anti-mouse immunoglobulin (Ig; 1:2,000; Millipore, no. 12-349), and polyclonal HRP-conjugated goat anti-rabbit Ig (1:2,000; Millipore, no. AP132P).

SDS-PAGE and immunoblotting. Transfected cells in six-well clusters were lysed to generate total cellular protein extracts using radioimmunoprecipitation assay lysis buffer (50 mM Tris-HCl [pH 7.4], 1% NP-40, 0.25% sodium deoxycholate, 150 mM NaCl, 1 mM EDTA) supplemented to contain 1% sodium dodecyl sulfate (SDS) and a cocktail of protease and phosphatase inhibitors (Sigma-Aldrich). Cells were rocked on ice for 15 min and centrifuged at 10,000 × *g* at 4°C for 10 min to remove cellular debris. Protein concentrations were determined by using a bicinchoninic acid (BCA) protein assay (Thermo Fisher Scientific). An aliquot of 10 to 30 μg of protein from each lysate was boiled for 5 min in 1× Laemmli sample buffer and resolved using 10% SDS-polyacrylamide gel electrophoresis (SDS-PAGE). The resolved proteins were transferred to nitrocellulose (Whatman; Protran, 0.45-μm pore size) in transfer buffer (48 mM Tris, 39 mM glycine, 0.04% SDS, 20% methanol) for 45 min at 15 V in a semidry transfer apparatus (Bio-Rad; Trans-Blot SD). Membranes were then blocked for 1 h with 3 to 5% milk or 5% bovine serum albumin (BSA; Sigma-Aldrich) in Tris-buffered saline (20 mM Tris-HCl [pH 7.6], 137 mM NaCl) containing 0.05 to 0.1% Tween 20 (TBS-T) and probed with the indicated primary antibodies at 4°C overnight. Membranes were washed three times with TBS-T buffer, followed by 90 min of incubation with the appropriate HRP-conjugated, species-specific secondary antibodies at room temperature. Membranes were washed, and proteins were visualized by using Amersham enhanced chemiluminescence (ECL) or ECL Plus kits (GE Healthcare) according to the manufacturer's instructions. Membranes were exposed to film and converted to digital format using an HP Scanjet G4050. Quantification of the digitized bands was determined using UN-SCAN-IT software (Silk Scientific).

Immunoprecipitation. Transfected cells in 6-well clusters were lysed using cell lysis buffer (Cell Signaling Technology) supplemented to contain a cocktail of protease and phosphatase inhibitors (Sigma-Aldrich). Cells were rocked on ice for 10 min, sonicated, and centrifuged at 14,000 × *g* at 4°C for 10 min to remove cellular debris. Protein concentrations were determined using a BCA protein assay. A portion (600 μg) of cell lysate was added to EZview Red anti-FLAG M2 affinity gel (Sigma-Aldrich) according to the manufacturer's instructions, followed by incubation at 4°C overnight while rotating. After centrifugation at 8,200 × *g* for 1 min, the supernatant was removed, and the beads were washed three times with ice-cold TBSX (20 mM Tris-HCl [pH 7.6], 137 mM NaCl, 2 mM ETDA, 1% Triton X-100). After the final wash, beads were resuspended in 50 μl of 2× Laemmli sample buffer lacking β-mercaptoethanol, boiled for 5 min, and centrifuged at 8,200 × *g* for 1 min. The supernatant was removed and subjected to SDS-PAGE (7.5% polyacrylamide gel).

Indirect immunofluorescence and confocal microscopy. Transfected Vero cells in 8-well collagen-coated chamber slides were fixed in 2% paraformaldehyde (Electron Microscopy Sciences) and permeabilized with 0.01% Triton X-100 in phosphate-buffered saline (PBS) at room temperature for 5 min. The slides were rinsed in PBS and blocked with 5% normal goat serum (Sigma-Aldrich) diluted in PBS at room temperature for 30 min. For DAPI (4′,6′-diamidino-2-phenylindole) staining, cells were incubated in 300 nM DAPI (Sigma, catalog no. D8417) diluted in PBS at room temperature for 15 min. The cells were incubated sequentially with rabbit polyclonal anti-μ2 antibody (1:600) and mouse monoclonal anti-Syk antibody (1:500; Millipore, catalog no. 05-434) or mouse anti-alpha tubulin (1:2,000; Sigma, catalog no. T6199) diluted in 0.01% IgG- and protease-free BSA (Jackson ImmunoResearch Laboratories, Inc.) for 30 min each. Samples were washed three times in PBS and incubated sequentially with Alexa 488- or Alexa 594-conjugated goat secondary antibodies (1:1,000; Invitrogen) for 30 min each to detect μ2, tubulin, and Syk. Samples were washed three times in PBS, and coverslips were mounted on slides using ProLong Gold reagent (Invitrogen). Images were captured using a Zeiss laser scanning confocal microscope model 710 equipped with a 40× C-apochromat/1.1 NA water immersion objective lens. The pinhole was maintained at 1 AU (40 μm), and images were taken using sequential scanning. Alexa Fluor 488 was excited at 488 nm using a multiline argon laser, and emission was detected in the 492- to 560-nm range. Alexa Fluor 594 was excited at 561 nm with a 561 diode pumped solid-state laser, and emission was detected in the 593- to 696-nm range. Images were processed and prepared for presentation using Adobe Photoshop CS4.

Quantification of viral replication. L929 cells, primary cardiac myocyte cultures, or AD-293 cells were plated in 96-well clusters and infected at the indicated multiplicity of infection (MOI). After incubation at 37°C for 1 h, additional media with or without anti-IFN-β antibody (640 neutralizing units/ml; PBL, catalog no. 32400-1) was added to each well, and the cells were incubated for various intervals with or without additional anti-IFN-β antibody (640 neutralizing units/ml at 2 days postinfection) before freezing at −80°C. Cells were subjected to two additional freeze-thaw cycles and subsequently lysed in 0.5% NP-40. Virus titers were determined by plaque assay using L929 cells (33).

Assessment of cytopathic effect. L929 cells or primary cardiac myocyte cultures were plated in 96-well clusters and infected with reovirus strains at various MOIs. After incubation at 37°C for 1 h, additional medium was added to each well. At 24 h, 5 days, or 7 days postinfection, cell viability was quantified by using an MTT assay (16). Absorbance was determined by subtracting the optical density (OD) at 650 nm from the

OD at 570 nm by using an automated microplate reader (Tecan Sunrise microplate reader).

Quantitative (real-time) reverse transcription-PCR (qRT-PCR). Cells in 24-well (L929 cells) or 48-well (primary cardiac myocyte cultures) clusters were infected with reovirus, incubated for 1 h, supplemented with medium, and then incubated for various intervals. Total RNA was harvested using an RNeasy kit (Qiagen) and treated with RNase-free DNase I (Qiagen). One-third of the RNA from each well was used to generate cDNA by reverse transcription in 100 μl containing 5 μM oligo(dT) (Invitrogen), 1× *Taq* buffer (Promega), 7.5 mM $MgCl_2$ (Promega), 1 mM dithiothreitol (Promega), 1 mM concentrations of each deoxynucleoside triphosphate (Roche), 0.67 U of RNasin (Promega)/μl, and 0.20 U of avian myeloblastosis virus (AMV) reverse transcriptase (Promega)/μl. Five percent (5 μl) of the resultant cDNA was amplified by using an iCycler iQ Real-Time PCR detection system (Bio-Rad Laboratories) in 96-well plates. Each duplicate 25-μl reaction mixture contained 1× Quantitech SYBR green master mix (Qiagen), 10 mM fluorescein, and 0.3 μM concentrations each of the forward and reverse primers. Primer sequences were previously described (34). The relative abundance of IFN-β and GAPDH (glyceraldehyde-3-phosphate dehydrogenase) mRNA was determined by comparison to a standard curve generated from serial dilutions of a DNA standard, and IFN-β expression was normalized to GAPDH expression.

Statistical analysis. A Student two-sample *t* test (pooled variance) was applied using Systat software. The results were considered significant if the *P* value was <0.05.

RESULTS

ITAM sequences are present in three reovirus proteins. The protein sequences encoded by each of the 10 reovirus gene segments were searched for potential ITAM sequences using the consensus motif YxxI/$Lx_{(6-12)}$YxxI/L (1). Remarkably, ITAM sequences were identified in three reovirus proteins: σ2 (amino acids [aa] 130 to 147), μ2 (aa 118 to 134), and λ2 (aa 671 to 684) encoded by the S2, M1, and L2 gene segments, respectively (Fig. 1A). ITAM sequences were not identified in a search of the related *Reoviridae* virus, rotavirus. ITAM sequences in the reovirus σ2, μ2, and λ2 proteins were identical among prototype strains type 1 Lang (T1L), type 2 Jones (T2J), and T3D. In addition, the sequences immediately adjacent to the ITAM sequences in all three reovirus proteins from T1L and T3D were identical and differed by only a few residues from T2J. A CLUSTAL alignment of the μ2 ITAM sequence with corresponding motifs from DAP12, FcRγ, and CD3ζ family members demonstrated conservation of the ITAM, as well as acidic residues in μ2 that are common to many cellular ITAMs (Fig. 1B). Conservation of critical residues in the motif across reovirus serotypes suggests a role for ITAMs in viral replication and pathogenesis. Given the previously established function of μ2 in modulating the IFN response and myocarditis in mice (29, 35), we first focused on the ITAM sequence in μ2.

μ2 is phosphorylated on tyrosine residues. Phosphorylation of conserved tyrosine residues is required for ITAM-mediated signaling (1). To determine whether the μ2 ITAM is equipped for similar signal transduction, we examined the phosphorylation status of μ2 tyrosine residues in FLAG-tagged μ2 and a derivative in which the two canonical ITAM tyrosine residues in μ2 were exchanged with phenylalanine residues (YYFF). Tyrosine-to-phenylalanine substitutions were chosen to prevent the phosphorylation required for ITAM function and to minimally alter protein structure given the similarity of the tyrosine and phenylalanine side chains. These substitutions did not compromise overall μ2 structure and function, as evidenced by the replication competence of similarly substituted whole recombinant viruses (see below). AD-293 cells were transfected with pFLAG-μ2, pFLAG-μ2-YYFF, or pFLAG-NS3/4A, which expresses the hepatitis C virus NS3/4A protein and was used as a negative control for tyrosine phosphorylation. Whole-cell lysates were immunoprecipitated using anti-FLAG antibody-conjugated beads, and fractions were resolved by SDS-PAGE and immunoblotted with anti-FLAG or anti-phosphotyrosine antibodies (Fig. 2). As expected, the anti-phosphotyrosine antibody did not detect FLAG-NS3/4A, although the protein was well expressed and immunoprecipitated. Notably, both FLAG-μ2 and FLAG-μ2-YYFF were tyrosine phosphorylated, providing the first evidence that μ2 is a phosphorylated protein. However, μ2 contains 30 tyrosines (36), and the significant phos-

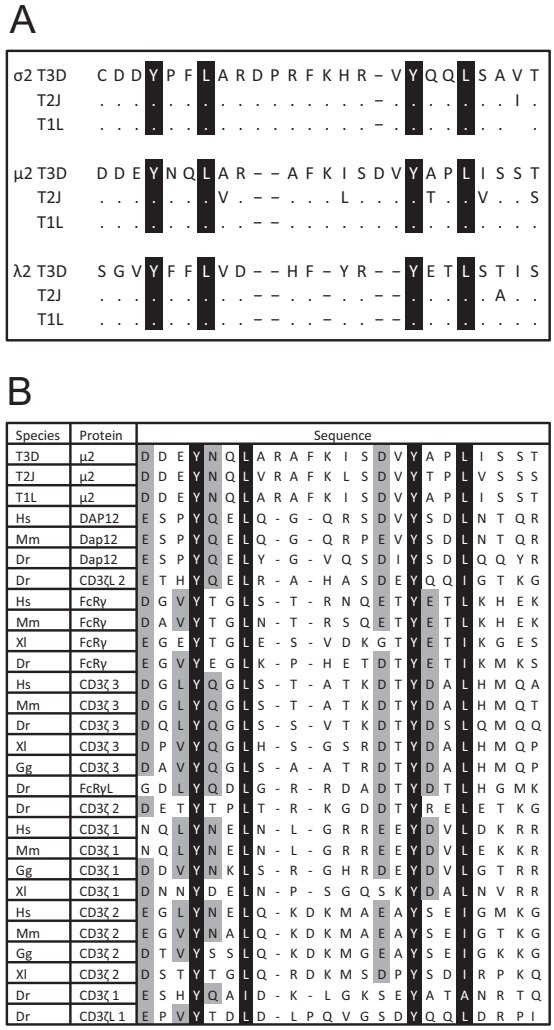

FIG 1 ITAM sequences are present in three reovirus proteins. (A) ITAMs in the reovirus σ2 (residues 127 to 151), μ2 (residues 115 to 138), and λ2 proteins (residues 668 to 688). ITAMs of prototype reovirus strains T3D, T2J, and T1L are shown. Sequences are from references 36, 63, and 64. Dots indicate identical residues and dashes indicate gaps in the alignment. (B) Reovirus μ2 ITAMs aligned with cellular ITAMs. Black indicates conserved ITAM residues. Gray indicates additional residues common to many ITAMs. Hs, *Homo sapiens* (human); Mm, *Mus musculus* (mouse); Dr, *Danio rerio* (zebrafish); Xl, *Xenopus laevis*; Gg, *Gallus gallus* (chicken). The extensions 1, 2, and 3 following protein names distinguish between the three ITAMs in each of the indicated proteins.

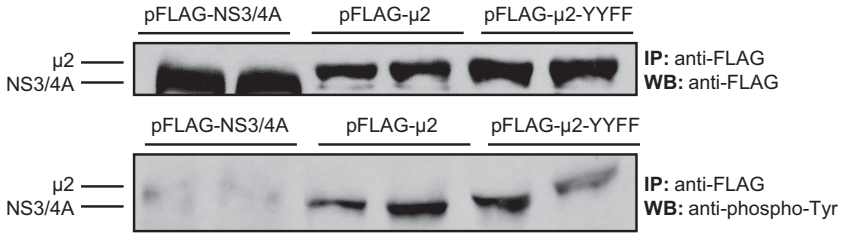

FIG 2 μ2 is phosphorylated on tyrosine residues. AD-293 cells were transfected with the indicated FLAG-tagged plasmid. At 40 h posttransfection, whole-cell lysates were immunoprecipitated using anti-FLAG beads, and fractions from duplicate samples were resolved by SDS-PAGE and immunoblotted with anti-FLAG or anti-phosphotyrosine antibodies. The results are representative of at least two independent experiments.

phorylation of FLAG-μ2-YYFF suggests that residues outside the ITAM sequence are phosphorylated. This abundant μ2 phosphorylation precluded detection of possible decreased phosphorylation in FLAG-μ2-YYFF relative to FLAG-μ2, leaving the status of tyrosine phosphorylation in the μ2 ITAM sequence unclear.

NF-κB is activated by μ2 and maximal activation requires the μ2 ITAM. NF-κB is a well-documented downstream target of ITAM-mediated signaling (7, 37), and reovirus activates NF-κB during infection (24, 25). To determine whether μ2 is capable of activating NF-κB, HEK-293 cells were transfected with pFLAG, pFLAG-μ2, or pFLAG-μ2-YYFF and, after 24 h, NF-κB-stimulated luciferase reporter gene expression was quantified (Fig. 3A). Transfected pFLAG-μ2 activated NF-κB, providing the first evidence that reovirus protein μ2 can activate this transcription factor. In sharp contrast, pFLAG-μ2-YYFF activation of NF-κB was minimal or undetectable, providing a direct biochemical link between the μ2 ITAM and NF-κB activation. As a control, μ2 expression levels in cell lysates generated from replicate cultures were quantified (Fig. 3B). Even when levels of FLAG-μ2-YYFF protein were >5-fold higher than the levels of FLAG-μ2 protein, pFLAG-μ2-YYFF activation of NF-κB was undetectable or significantly less than that by pFLAG-μ2 (compare 1 μg of pFLAG-μ2-YYFF to 0.1 μg of pFLAG-μ2, with average band intensities of 200 and 40, respectively, in Fig. 3B, to the relative activations of NF-κB at those concentrations in Fig. 3A). Finally, neither pFLAG-μ2 nor pFLAG-μ2-YYFF induced IFN-β or the IFN-stimulated pathway as assessed by an ISRE reporter (Fig. 3A). These results are consistent with a requirement for viral activation of IRF3 for induction of IFN-β, suggest that μ2 alone cannot activate IRF3, and highlight the specific effect of the μ2 ITAM on activation of NF-κB.

μ2 requires Syk for maximal activation of NF-κB. ITAM-mediated activation of NF-κB requires Syk (or Zap-70 in T cells) (3, 38). To determine whether Syk is required for μ2-mediated activation of NF-κB, AD-293 cells were pretreated with DMSO alone or with the Syk-specific inhibitor piceatannol before transfection with plasmids encoding either FLAG-tagged or untagged μ2 (Fig. 4A). After 24 h, NF-κB-stimulated luciferase reporter gene expression was quantified. Piceatannol decreased μ2 activation of NF-κB 2.5- to 2.9-fold, demonstrating a requirement for Syk in maximal μ2-mediated signal transduction. μ2 was expressed at equivalent levels in DMSO- and piceatannol-treated lysates (Fig. 4B), demonstrating that reduced μ2 activation of NF-κB is due to inhibition of Syk activity rather than decreased μ2 expression. Thus, μ2 contains a functional ITAM that signals through an established ITAM-associated signaling intermediate to activate NF-κB.

μ2 and μNS recruit Syk to viral factories and recruitment requires the μ2 ITAM. Reovirus protein μ2 does not span membranes, suggesting it functions in a manner that differs from other viral and cellular ITAM-containing proteins (1, 8). Although μ2 is found in low copy numbers within the viral core, μ2 is abundant and highly concentrated in reovirus-infected cells within cytoplasmic viral replication-associated VFs, also known as viral inclusion bodies (VIBs) (15, 39). Although VFs are thought to lack a delimiting membrane, we hypothesized that these structures may serve as intracellular sites for μ2 ITAM interaction with Syk. Transfection of plasmids expressing reovirus proteins μNS and μ2 is sufficient to induce formation of VF-like structures, but the VF morphology is determined by the μ2 allele. T3D-derived μ2 generates globular VFs, whereas T1L-derived μ2 generates filamentous VFs (39, 40). To determine the effect of the μ2 ITAM on Syk subcellular localization, we used confocal microscopy to examine transfected Vero cells, which have larger cytoplasms and more defined VFs than do AD-293 cells. Cells cotransfected with pFLAG-μ2 and GFP-μNS generated globular VFs as expected, whereas cells transfected with pFLAG-μ2-YYFF and GFP-μNS generated VFs with an intermediate morphology (Fig. 5A). As expected, pFLAG-μ2-YYFF was similar to the parental T3D-derived pFLAG-μ2 in its failure to colocalize with microtubules, in contrast to a T1L-derived HA-tagged μ2 (Fig. 5B). In cells cotransfected with plasmids expressing Syk, μNS and pFLAG or pFLAG-μ2-YYFF (Fig. 5C), Syk remained diffuse throughout the cell, despite adequate formation of VFs in the latter. Conversely, in cells transfected with Syk, μNS and pFLAG-μ2, Syk was localized to VFs. Thus, μ2 and μNS recruit Syk to VFs and recruitment requires the μ2 ITAM, representing a new mechanism for viral ITAM-mediated signaling.

The μ2 ITAM regulates activation of NF-κB during viral infection. To determine whether reovirus ITAM sequences function during viral infection, plasmid-based reverse genetics was used to engineer WT reovirus strain T3D and several mutant viruses. Mutant viruses with altered ITAMs in the λ2 protein could not be recovered despite three independent rescue attempts. However, viruses with altered σ2 (σ2-YYFF) or μ2 (μ2-YYFF) ITAMs were readily isolated and formed plaques similar in size to WT virus (data not shown). To determine whether the μ2 ITAM regulates activation of NF-κB in the context of reovirus infection, AD-293 cells were cotransfected with the NF-κB-luciferase reporter plasmid and *Renilla* luciferase plasmid prior to infection with WT T3D, σ2-YYFF, or μ2-YYFF viruses. At 12 h postinfection, WT T3D and σ2-YYFF viruses activated NF-κB, but μ2-YYFF did not (Fig. 6A). Although μ2-YYFF achieved a titer higher than that of σ2-YYFF virus at 12 h postinfection (Fig. 6B), it remained possible that differences in NF-κB activation might reflect differences in

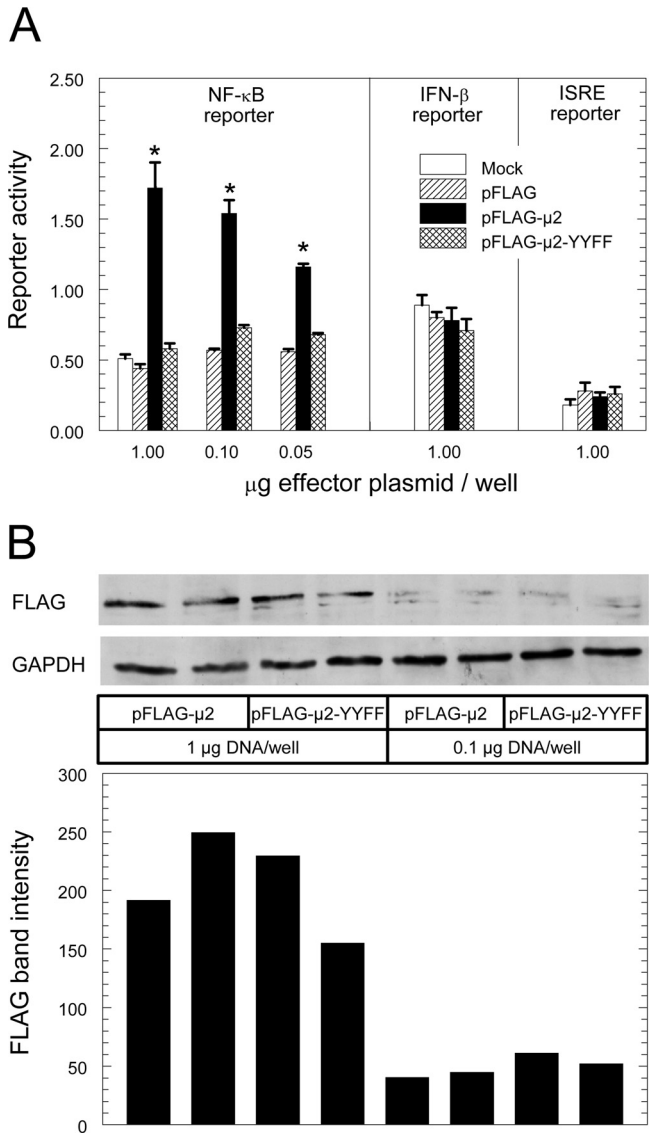

FIG 3 NF-κB is activated by μ2 and maximal activation requires the μ2 ITAM. (A) HEK-293 cells were cotransfected with the indicated FLAG-tagged plasmid, a constitutively expressing *Renilla* luciferase plasmid for normalizations, and a luciferase reporter plasmid regulated by NF-κB, IFN-β, or ISRE promoters. At 24 h posttransfection, luciferase activity was quantified. The results are expressed as means ± the standard errors of the mean of five replicate samples and are representative of two independent experiments. (B) Whole-cell lysates corresponding to panel A were resolved by SDS-PAGE, transferred to a nitrocellulose membrane, and immunoblotted with anti-FLAG or anti-GAPDH antibodies. Gels were scanned, and band intensities were quantified. The results are presented as the FLAG intensity normalized to the GAPDH intensity and are representative of at least two independent experiments. *, Significantly different from pFLAG and pFLAG-μ2-YYFF ($P < 0.05$).

replication. However, even at 24 h postinfection when μ2-YYFF achieved titers comparable to those of WT T3D and σ2-YYFF (Fig. 6B), μ2-YYFF failed to activate NF-κB as efficiently as either virus (Fig. 6A). Therefore, decreased activation of NF-κB by reovirus mutant μ2-YYFF is not attributable to diminished viral replication, but instead reflects the requirement for the μ2 ITAM for maximal activation of NF-κB during reovirus infection.

The μ2 ITAM regulates induction of IFN-β. Viral activation of NF-κB is required for maximal induction of IFN-β, and the IFN-β response is a critical determinant of protection against reovirus-induced myocarditis in mice (16, 35, 41). Moreover, the M1 gene (encoding the μ2 protein) is the predominant determinant of reovirus induction of IFN-β in primary cardiac myocyte cultures (16). To determine whether the μ2 ITAM regulates reovirus induction of IFN-β, primary cardiac myocyte cultures and a control fibroblast-derived L929 cell line were infected with WT T3D and mutant reoviruses, and induction of IFN-β mRNA was quantified. The σ2-YYFF virus induced less IFN-β in L929 cells than did WT T3D (Fig. 7A), perhaps due to its poorer replication than WT T3D (Fig. 7B). In contrast, in both L929 cells and primary cardiac myocyte cultures, μ2-YYFF induced significantly less IFN-β than did either WT T3D or σ2-YYFF viruses (Fig. 7A), despite replicating to similar or higher titers (Fig. 7B). Thus, the μ2 ITAM regulates induction of IFN-β.

The μ2 ITAM effect on viral spread is cell type specific. Viral spread is determined by viral replication, virus-induced cytopathicity for virus release, and the effect of virus-induced antiviral cytokines. The role of reovirus-activated NF-κB in these processes is cell type specific. NF-κB is required for reovirus-induced apoptosis in most cell types but not in cardiac myocytes (26). Accordingly, NF-κB is required for reovirus-induced apoptosis and damage in the brain, whereas in the heart, where IFN-β is critical in limiting viral spread, NF-κB is predominantly antiviral (16, 18, 35). To determine the effect of the μ2 ITAM on viral spread, L929 cells and primary cardiac myocyte cultures were infected at a low MOI with WT T3D, σ2-YYFF, or μ2-YYFF viruses and then incubated for 5 to 7 days to allow multiple cycles of viral replication. In L929 cells, all three viruses achieved equivalent virus titers (Fig. 8A). However, μ2-YYFF was significantly less cytopathic than either WT T3D or σ2-YYFF viruses at both 5 and 7 days postinfection (Fig. 9). These results suggest that in fibroblasts, where NF-κB is required for reovirus-induced apoptosis (25), the μ2 ITAM is advantageous for viral spread. In contrast to L929 cells, μ2-YYFF achieved significantly higher titers than either WT T3D or σ2-YYFF viruses in primary cardiac myocyte cultures (Fig. 8A). Inclusion of anti-IFN-β antibody during infection increased replication of both WT T3D and σ2-YYFF viruses to levels similar to that of μ2-YYFF in cardiac myocyte cultures but had no effect on the virus titer in L929 cells (Fig. 8B). Thus, the effect of the μ2 ITAM on viral spread is mediated by the IFN-β response and is cell type specific. Finally, again in contrast to L929 cells, μ2-YYFF was significantly more cytopathic than either WT T3D or σ2-YYFF in primary cardiac myocyte cultures (Fig. 9). Therefore, in cardiac myocytes, where the IFN response is required to limit viral damage and NF-κB is not required for apoptosis (16–18, 26), the μ2 ITAM stimulates cellular defense mechanisms and diminishes viral replication and spread. Thus, the effect of the μ2 ITAM on reovirus replication and cytopathology is cell type specific.

DISCUSSION

Viral infections evoke a variety of cellular responses that can either promote or antagonize viral replication. We report here that the reovirus M1 gene-encoded μ2 protein contains a functional ITAM that regulates activation of NF-κB and induction of IFN-β and that the benefit of the ITAM to the virus is cell type specific. Furthermore, we provide evidence of a new mechanism for viral ITAM-mediated signaling by a nonenveloped virus.

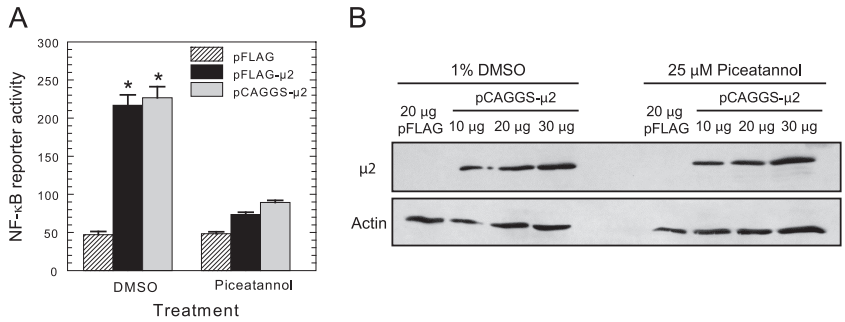

FIG 4 μ2 requires Syk for maximal activation of NF-κB. (A) AD-293 cells were treated for 1 h with DMSO alone or 25 μM the Syk-specific inhibitor piceatannol and then cotransfected with the indicated effector plasmid, a constitutively expressing *Renilla* luciferase plasmid for normalizations, and an NF-κB-luciferase reporter plasmid. At 24 h posttransfection, the luciferase activity was quantified. The results are expressed as means plus the standard errors of the mean of six replicate samples and are representative of at least two independent experiments. (B) The indicated amount (in μg) of whole-cell lysates corresponding to panel A were resolved by SDS-PAGE, transferred to a nitrocellulose membrane, and immunoblotted with anti-μ2 or anti-actin-HRP antibodies. The results are representative of at least two independent experiments. *, Significantly different from pCAGGS-μ2 and pFLAG-μ2 in piceatannol and pFLAG in either treatment ($P < 0.02$).

The two critical tyrosine residues within the canonical ITAM motif YxxI/Lx$_{(6-12)}$YxxI/L must be phosphorylated for the efficient recruitment of Syk tyrosine kinases and the activation of ITAM-mediated signaling cascades (1). In the present study, we demonstrate that μ2 undergoes tyrosine phosphorylation, providing the first evidence that μ2 is a phosphorylated protein (Fig. 2). Phosphorylation of the critical ITAM tyrosine residues remains unclear.

ITAM tyrosine phosphorylation is dependent on Src family kinase members, including Src, Lck, Lyn, Fgr, Hck, Fyn, and Yes, some of which are expressed in only certain cell types (38). Furthermore, viral ITAMs display cell type-specific kinase associations. The SIV Nef protein ITAM associates with Src in 3T3 cells (42) and yet requires Lck binding in Jurkat cells (43). The Epstein-Barr virus (EBV) LMP2A ITAM is phosphorylated by Csk in epithelial cells but preferentially associates with Lyn and Fyn in BJAB cells, a B cell line (44, 45). Reovirus infects a wide variety of tissues *in vivo*, including the brain, heart, liver, intestine, and spleen (15). Future investigations will determine whether the association of Src family kinases with the μ2 ITAM varies between cell types and influences the capacity of the μ2 ITAM to modulate cell signaling.

We found that NF-κB, a well-documented downstream target of ITAM-mediated signaling (1, 7), is activated by μ2 and that maximal activation requires the μ2 ITAM (Fig. 3). In addition, ectopically expressed μ2 does not activate IFN-β or ISRE luciferase reporters (Fig. 3). Together, our results are consistent with the requirement for the protein MAVS (IPS-1) for reovirus activation of transcription factor IRF3 but not NF-κB (17). Although previous investigations have demonstrated that reovirus outer-capsid protein μ1 activates NF-κB (46–48), results presented here for μ2 suggest reovirus regulates NF-κB activation through multiple viral effectors. Reovirus NF-κB activation requires components of both the classical and alternative NF-κB signaling pathways in an integrated mechanism involving IKKα and the IKKβ regulatory protein NEMO/IKKγ but not IKKβ or the IKKα activator NIK (49). It has been hypothesized that the φ domain of reovirus protein μ1 contributes to NF-κB activation through direct or indirect stimulation of IKKs in a fashion similar to that seen during human T-lymphotropic virus (HTLV) infection, in which the HTLV Tax protein stimulates IKK activity through direct interaction with NEMO/IKKγ (48). Activation of NF-κB by μ2 instead requires ITAM-mediated signaling intermediates.

We demonstrate that μ2 requires Syk for maximal activation of NF-κB (Fig. 4), providing evidence that μ2 contains a functional ITAM that signals through an established ITAM-associated signaling intermediate. Syk tyrosine kinases mediate signal transduction for several viral ITAMs, including EBV LMP2A (50), Kaposi's sarcoma-associated herpesvirus (KSHV) K1 (51, 52), mouse mammary tumor virus (MMTV) envelope protein (Env) (53), hantavirus G1 (9, 54), and SIV Nef (10, 43). LMP2A is a highly hydrophobic protein containing 12 transmembrane domains and is localized in clusters within the plasma membrane of latently infected B cells. The recruitment of kinases to LMP2A ITAM residues for tyrosine phosphorylation is stimulated by cellular adhesion rather than ligand binding as classically demonstrated by ITAM-associated proteins (44). The KSHV K1 ITAM is located within the cytoplasmic tail of this transmembrane protein and can constitutively induce signal transduction through ligand-independent activation attributable to the K1 cysteine-rich extracellular domain (12, 55). However, reovirus is a nonenveloped virus, and μ2 does not span cellular membranes, suggesting that it must stimulate Syk by a previously undescribed mechanism. The structure of μ2 has not been determined, but the ITAM identified here is located directly adjacent to a μ2 sequence predicted to have the greatest likelihood of localization to the protein surface, a finding consistent with a model of direct interaction between the μ2 ITAM and the Syk SH2 domain (36).

Replication and assembly of reovirus progeny occurs within cytoplasmic VFs, also known as VIBs. Reovirus protein μNS initiates VF formation by establishing a structural matrix and acting as a scaffolding protein for recruitment of μ2, S3-encoded nonstructural protein σNS, and core structural proteins (40, 56, 57). VFs become tethered to the cellular cytoskeleton via μNS associations with the microtubule-associated μ2. This association allows VFs to travel toward the nucleus and merge with other VFs, ultimately forming the large perinuclear inclusions characteristic of reovirus-infected cells (39, 56). We found that μ2 and μNS, major components of VFs, recruit Syk to viral factories and that the μ2 ITAM is required for this translocation (Fig. 5). Syk phosphorylates microtubules (58), and reovirus strain T1L protein μ2

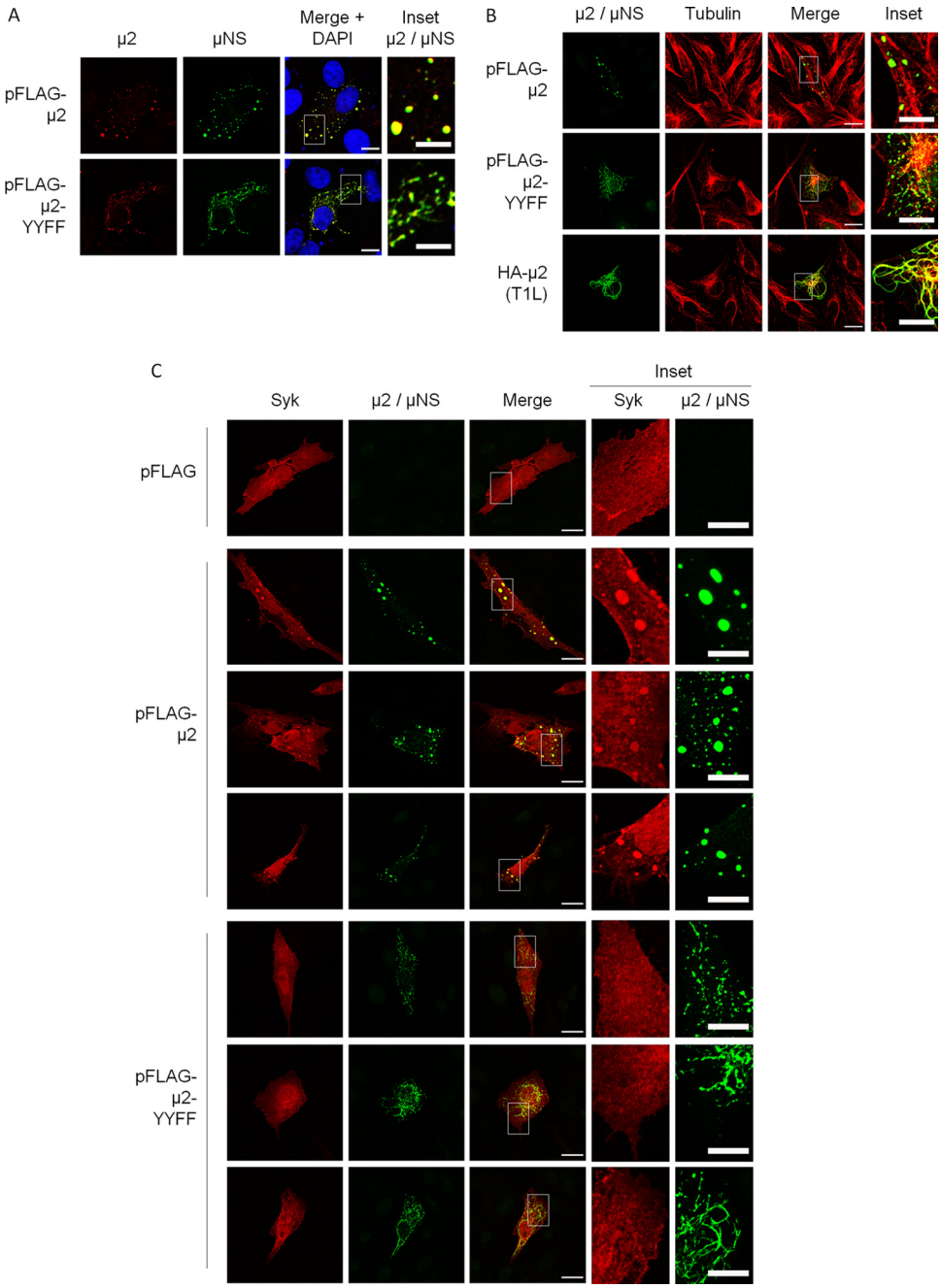

FIG 5 μ2 and μNS recruit Syk to viral factories and recruitment requires the μ2 ITAM. Vero cells were cotransfected with the indicated plasmids. At 24 h posttransfection, the cells were fixed and immunostained, and nuclei were stained with DAPI. (A) Cells were transfected with GFP-μNS (green) and the indicated μ2-expressing plasmid and then immunostained with anti-μ2 antibody (red). (B) Cells were transfected as in panel A and immunostained with anti-μ2 (green) and anti-tubulin (red) antibodies. (C) Cells were transfected as in panel A with the addition of a Syk-expressing plasmid and immunostained with anti-Syk (red) and anti-μ2 (green) antibodies. The results are representative of three independent experiments. Scale bar, 20 μm; inset scale bar, 10 μm.

binds microtubules (40). As expected, the T3D-derived μ2-YYFF fails to colocalize with microtubules. Future investigations will address whether microtubules function in μ2 ITAM-Syk interactions. Furthermore, while VFs are thought to lack a delimiting membrane, further studies of the structural composition of VFs may identify properties of VFs that support μ2 ITAM-Syk interaction.

During reovirus infection, NF-κB plays a proapoptotic role in the brain stimulating neuronal apoptosis, while in the heart NF-κB is not required for apoptosis and instead leads to induction of innate immune mediators, including IFN-β (18). We found that the μ2 ITAM is required for maximal activation of NF-κB and induction of IFN-β in both L929 cells and primary cardiac myocyte cultures (Fig. 7) but that the consequences to viral cytopathic effect and spread are cell type specific (Fig. 8 and 9). Together, these data suggest that in fibroblasts where NF-κB is re-

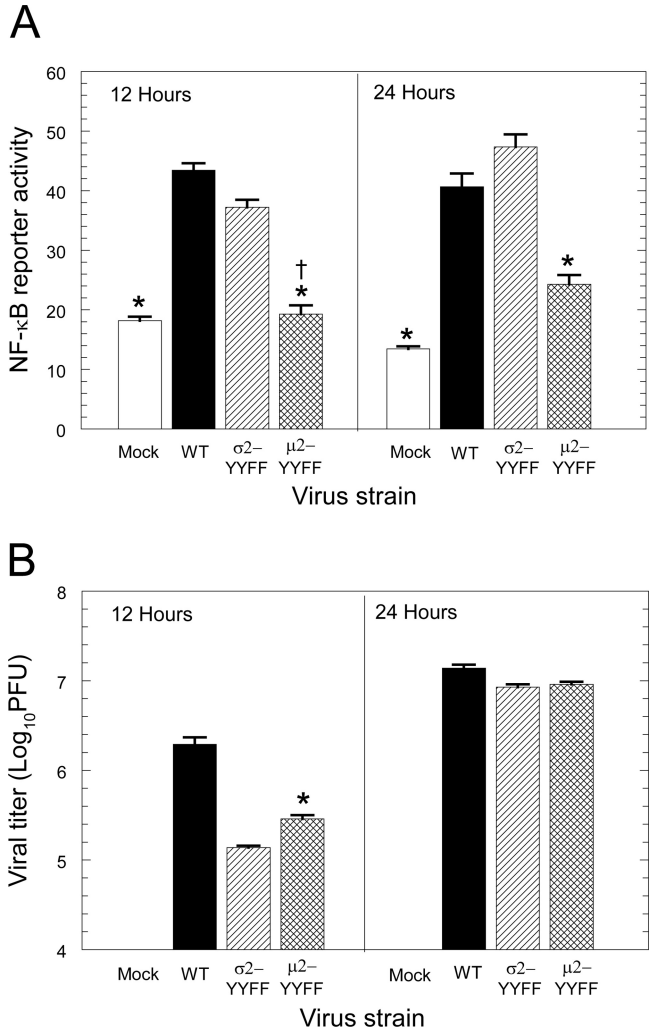

FIG 6 The μ2 ITAM regulates activation of NF-κB during viral infection. (A) AD-293 cells were transfected with an NF-κB-luciferase reporter plasmid and a constitutively expressing *Renilla* luciferase plasmid for normalizations. At 24 h posttransfection, cells were infected with the indicated virus at an MOI of 10 PFU per cell. At 12 and 24 h postinfection, the luciferase activity was quantified. The results are expressed as means ± the standard deviations of four or five replicate wells and are representative of at least three independent experiments. (B) AD-293 cells were infected with the indicated virus at an MOI of 3 PFU per cell. At 12 and 24 h postinfection, the virus titers were determined by plaque assay. The results are expressed as the means of quadruplicate samples plus the standard deviations for a representative of at least two independent experiments. *, Significantly different from WT T3D and σ2-YYFF ($P < 0.05$); †, not significantly different from mock ($P > 0.05$).

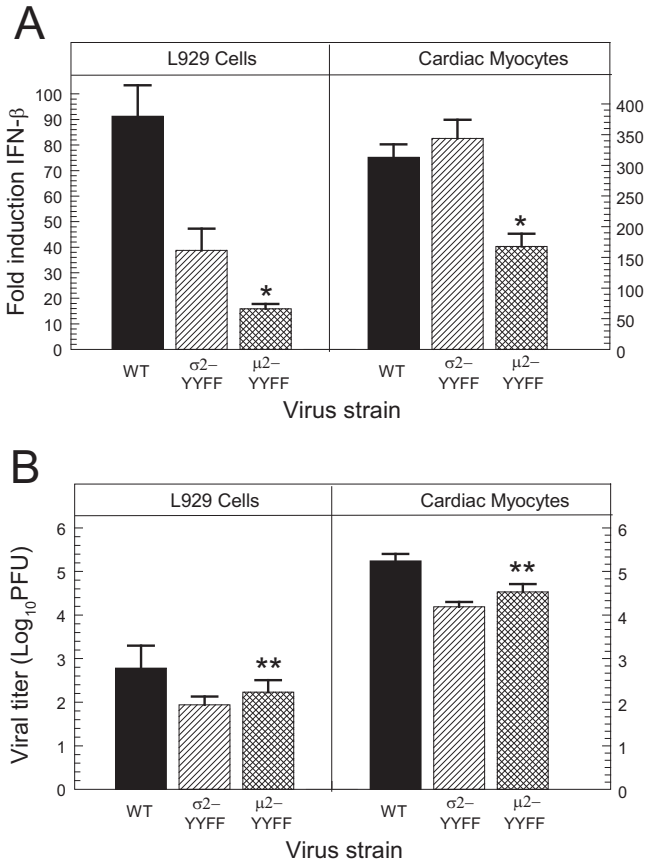

FIG 7 The μ2 ITAM regulates induction of IFN-β during viral infection. (A) L929 cells or primary cardiac myocyte cultures were infected at an MOI of 25 or 10 PFU per cell, respectively. At 8 or 12 h postinfection, RNA was quantified by reverse transcription and quantitative real-time PCR, and the copy number was normalized to GAPDH. The fold induction of IFN-β is expressed relative to mock-infected cultures. The results are expressed as means ± the standard errors of the mean of triplicate wells for a representative of three independent experiments. (B) L929 cells or primary cardiac myocytes cultures were infected with the indicated virus at an MOI of 3 PFU per cell. At 8 h postinfection, the virus titers were determined by plaque assay. The results are expressed as means plus the standard deviations for two or three independent experiments each with triplicate wells. *, Significantly different from WT T3D and σ2-YYFF ($P < 0.05$); **, significantly different from σ2-YYFF ($P < 0.05$).

quired for reovirus-induced apoptosis, as it is in most cell types (25), the μ2 ITAM is advantageous for viral spread and enhances viral fitness. In cardiac myocytes, where IFN-β is essential for protection against reovirus replication and cytopathology (16–18) and NF-κB is not required for apoptosis (26), the μ2 ITAM stimulates cellular defense mechanisms and thereby diminishes viral fitness.

Several enveloped viruses encode ITAM-bearing proteins that signal through traditional cellular ITAM signaling intermediates to regulate viral pathogenesis and oncogenesis (8). During EBV infection, Syk regulates LMP2A ITAM-induced epithelial cell migration through activation of MAPK extracellular signal-regulated kinase (ERK) (50). This ITAM-bearing protein also is essential for ERK-mediated reduction of anoikis, a type of apoptosis associated with cell detachment (59). Finally, LMP2A ITAM-mediated Syk autophosphorylation initiates activation of Akt, a serine/threonine protein kinase that contributes to B cell survival and is required for LMP2A-induced transformation of epithelial cells (60). In the KSHV K1 ITAM, each tyrosine residue targets distinct SH2-containing proteins, including phosphatidylinositol 3-kinase, PLCγ2, and Vav. These interactions lead to regulated augmentation of signal transduction activities involved in Kaposi's sarcoma hyperplasia, such as intracellular calcium mobilization, the activation of transcription factors NFAT and AP-1, and the production of inflammatory cytokines and angiogenic growth factors (52). In addition, the SIV Nef ITAM is necessary and sufficient for Lck activation of NFAT, a key downstream intermediate of T cell activation (10, 43). Although the results reported here demonstrate that the μ2 ITAM stimulates Syk activation of NF-

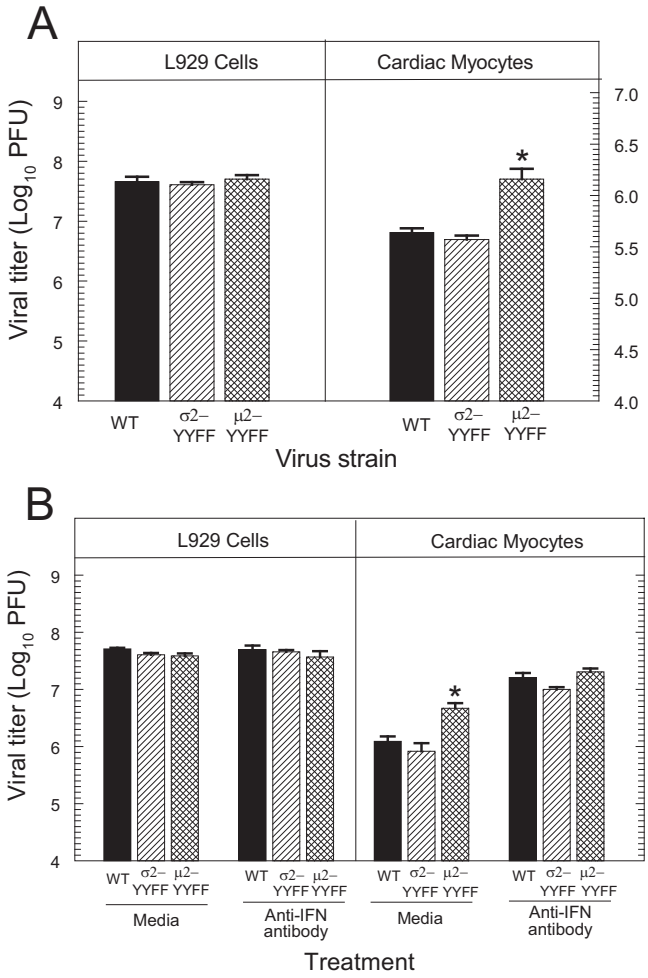

FIG 8 The effect of the μ2 ITAM on virus titer after multiple cycles of replication is cell type specific and was determined by the IFN-β response. (A) L929 cells and primary cardiac myocyte cultures were infected with the indicated virus at an MOI of 0.1 PFU per cell. At 5 days postinfection, the virus titers were determined by plaque assay. The results are expressed as means ± the standard deviations of triplicate wells for a representative of at least two independent experiments. (B) L929 cells and primary cardiac myocyte cultures were infected at an MOI of 0.1 or 0.3 PFU per cell, respectively. At 1 h postinfection, inocula were removed and replaced with either medium alone or medium containing anti-IFN-β antibody. At 2 days postinfection, additional anti-IFN-β antibody was added to appropriate wells. The results are expressed as the means of quadruplicate samples plus the standard deviations for a representative of at least two independent experiments. *, Significantly different from WT T3D and σ2-YYFF ($P < 0.05$).

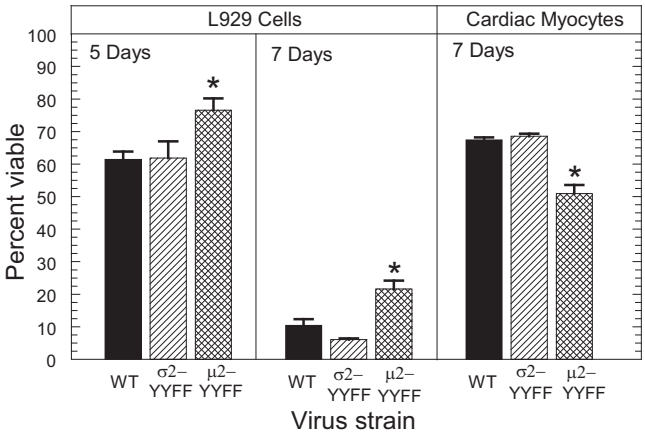

FIG 9 The effect of the μ2 ITAM on cytopathic effect after multiple cycles of replication is cell type specific. L929 cells or primary cardiac myocyte cultures were infected with the indicated virus at an MOI of 0.1 or 1 PFU/cell, respectively (the cytopathic effect was undetectable in cardiac myocytes infected at 0.1 PFU/cell; data not shown). At 5 and 7 days postinfection, the cell viability was quantified by using an MTT assay. The results from a minimum of four replicate wells per infection are expressed as the means plus the standard errors of the mean relative to mock-infected cultures for a representative of at least two independent experiments. *, Significantly different from WT T3D and σ2-YYFF ($P < 0.05$).

κB, μ2-stimulated Syk also may activate other transcription factors.

Although viral ITAMs are most often associated with oncogenesis (11, 52, 53, 60–62), reovirus is not oncogenic. There are two nononcogenic viruses known to encode ITAM-containing proteins: hantavirus and SIV. The hantavirus G1 ITAM is highly conserved in hantavirus strains causing hantavirus pulmonary syndrome but absent in those causing hemorrhagic fever with renal syndrome or nonpathogenic strains, suggesting that this viral ITAM is a determinant of pathogenesis. In SIV, the primary pathogenic determinant of a highly virulent isolate was identified to be an arginine to tyrosine mutation within Nef that causes Nef to express a functional ITAM (10, 43). The cell type-specific effects of the reovirus μ2 ITAM identified here suggest that it is likely to be a determinant of pathogenesis *in vivo*, and the capacity of reovirus to target a variety of organs in mice offers an excellent opportunity for discovery. As a final note, an ITAM-like sequence has been identified in only one nonenveloped virus to date: coxsackievirus. However, substitution of critical tyrosine residues within the ITAM-like region of capsid protein VP2 severely attenuated the virus, leaving interpretation of the results presented on ITAM function unclear (14).

Our findings define a new role for reovirus protein μ2, enhance our understanding of reovirus activation of NF-κB and induction of IFN-β, and provide additional evidence for cell type-specific downstream effects of NF-κB during viral infection. Furthermore, we provide here the first evidence for a functional ITAM in a nonenveloped virus and present a new mechanism for viral ITAM-mediated signaling.

ACKNOWLEDGMENTS

We thank Ralph Baric, Lianna Li, Kim Parks, Ray Pickles, Frank Scholle, and Jennifer Zurney for helpful discussions and Lance Johnson for excellent technical assistance.

This research was supported by Public Health Service awards T32 CA09385 (K.W.B.), F32 AI075776 (K.W.B.), R37 AI38296 (T.S.D.), R01 AI50080 (T.S.D.), and R01 A1083333 (B.S.), a U.S. Department of Education Graduate Assistance in Areas of National Need (GAANN) Fellowship (E.E.R.-S.), and the Elizabeth B. Lamb Center for Pediatric Research. Additional support was provided by Public Health Service awards CA68485 for the Vanderbilt-Ingram Cancer Center and DK20593 for the Vanderbilt Diabetes Research and Training Center.

REFERENCES

1. **Underhill DM, Goodridge HS.** 2007. The many faces of ITAMs. Trends Immunol. **28:**66–73. http://dx.doi.org/10.1016/j.it.2006.12.004.
2. **Berton G, Mocsai A, Lowell CA.** 2005. Src and Syk kinases: key regulators

of phagocytic cell activation. Trends Immunol. **26:**208–214. http://dx.doi.org/10.1016/j.it.2005.02.002.
3. **Mocsai A, Ruland J, Tybulewicz VL.** 2010. The SYK tyrosine kinase: a crucial player in diverse biological functions. Nat. Rev. Immunol. **10:**387–402. http://dx.doi.org/10.1038/nri2765.
4. **Sada K, Takano T, Yanagi S, Yamamura H.** 2001. Structure and function of Syk protein-tyrosine kinase. J. Biochem. **130:**177–186. http://dx.doi.org/10.1093/oxfordjournals.jbchem.a002970.
5. **Barrow AD, Trowsdale J.** 2006. You say ITAM and I say ITIM, let's call the whole thing off: the ambiguity of immunoreceptor signaling. Eur. J. Immunol. **36:**1646–1653. http://dx.doi.org/10.1002/eji.200636195.
6. **Humphrey MB, Lanier LL, Nakamura MC.** 2005. Role of ITAM-containing adapter proteins and their receptors in the immune system and bone. Immunol. Rev. **208:**50–65. http://dx.doi.org/10.1111/j.0105-2896.2005.00325.x.
7. **Hara H, Ishihara C, Takeuchi A, Xue L, Morris SW, Penninger JM, Yoshida H, Saito T.** 2008. Cell type-specific regulation of ITAM-mediated NF-κB activation by the adaptors, CARMA1 and CARD9. J. Immunol. **181:**918–930. http://www.jimmunol.org/content/181/2/918.full.
8. **Lanier LL.** 2006. Viral immunoreceptor tyrosine-based activation motif (ITAM)-mediated signaling in cell transformation and cancer. Trends Cell Biol. **16:**388–390. http://dx.doi.org/10.1016/j.tcb.2006.06.004.
9. **Geimonen E, LaMonica R, Springer K, Farooqui Y, Gavrilovskaya IN, Mackow ER.** 2003. Hantavirus pulmonary syndrome-associated hantaviruses contain conserved and functional ITAM signaling elements. J. Virol. **77:**1638–1643. http://dx.doi.org/10.1128/JVI.77.2.1638-1643.2003.
10. **Dehghani H, Brown CR, Plishka R, Buckler-White A, Hirsch VM.** 2002. The ITAM in Nef influences acute pathogenesis of AIDS-inducing simian immunodeficiency viruses SIVsm and SIVagm without altering kinetics or extent of viremia. J. Virol. **76:**4379–4389. http://dx.doi.org/10.1128/JVI.76.9.4379-4389.2002.
11. **Beaufils P, Choquet D, Mamoun RZ, Malissen B.** 1993. The (YXXL/I)2 signaling motif found in the cytoplasmic segments of the bovine leukaemia virus envelope protein and Epstein-Barr virus latent membrane protein 2A can elicit early and late lymphocyte activation events. EMBO J. **12:**5105–5112.
12. **Lee H, Guo J, Li M, Choi JK, DeMaria M, Rosenzweig M, Jung JU.** 1998. Identification of an immunoreceptor tyrosine-based activation motif of K1 transforming protein of Kaposi's sarcoma-associated herpesvirus. Mol. Cell. Biol. **18:**5219–5228.
13. **Katz E, Lareef MH, Rassa JC, Grande SM, King LB, Russo J, Ross SR, Monroe JG.** 2005. MMTV Env encodes an ITAM responsible for transformation of mammary epithelial cells in three-dimensional culture. J. Exp. Med. **201:**431–439. http://dx.doi.org/10.1084/jem.20041471.
14. **Kim DS, Park JH, Kim JY, Kim D, Nam JH.** 2012. A mechanism of immunoreceptor tyrosine-based activation motif (ITAM)-like sequences in the capsid protein VP2 in viral growth and pathogenesis of coxsackievirus B3. Virus Genes **44:**176–182. http://dx.doi.org/10.1007/s11262-011-0681-x.
15. **Dermody TS, Parker J, Sherry B.** 2013. Orthoreoviruses, p 1304–1346. *In* Knipe DM, Howley PM (ed), Fields virology, 6th ed. Lippincott/The Williams & Wilkins Co, Philadelphia, PA.
16. **Sherry B, Torres J, Blum MA.** 1998. Reovirus induction of and sensitivity to beta interferon in cardiac myocyte cultures correlate with induction of myocarditis and are determined by viral core proteins. J. Virol. **72:**1314–1323.
17. **Holm GH, Pruijssers AJ, Li L, Danthi P, Sherry B, Dermody TS.** 2010. Interferon regulatory factor 3 attenuates reovirus myocarditis and contributes to viral clearance. J. Virol. **84:**6900–6908. http://dx.doi.org/10.1128/JVI.01742-09.
18. **O'Donnell SM, Hansberger MW, Connolly JL, Chappell JD, Watson MJ, Pierce JM, Wetzel JD, Han W, Barton ES, Forrest JC, Valyi-Nagy T, Yull FE, Blackwell TS, Rottman JN, Sherry B, Dermody TS.** 2005. Organ-specific roles for transcription factor NF-κB in reovirus-induced apoptosis and disease. J. Clin. Invest. **115:**2341–2350. http://dx.doi.org/10.1172/JCI22428.
19. **Sherry B, Schoen FJ, Wenske E, Fields BN.** 1989. Derivation and characterization of an efficiently myocarditic reovirus variant. J. Virol. **63:**4840–4849.
20. **Sherry B, Blum MA.** 1994. Multiple viral core proteins are determinants of reovirus-induced acute myocarditis. J. Virol. **68:**8461–8465.
21. **Zurney J, Howard KE, Sherry B.** 2007. Basal expression levels of IFNAR and Jak-STAT components are determinants of cell-type-specific differences in cardiac antiviral responses. J. Virol. **81:**13668–13680. http://dx.doi.org/10.1128/JVI.01172-07.
22. **Kato H, Takeuchi O, Mikamo-Satoh E, Hirai R, Kawai T, Matsushita K, Hiiragi A, Dermody TS, Fujita T, Akira S.** 2008. Length-dependent recognition of double-stranded ribonucleic acids by retinoic acid-inducible gene-I and melanoma differentiation-associated gene 5. J. Exp. Med. **205:**1601–1610. http://dx.doi.org/10.1084/jem.20080091.
23. **Loo YM, Fornek J, Crochet N, Bajwa G, Perwitasari O, Martinez-Sobrido L, Akira S, Gill MA, Garcia-Sastre A, Katze MG, Gale M, Jr.** 2008. Distinct RIG-I and MDA5 signaling by RNA viruses in innate immunity. J. Virol. **82:**335–345. http://dx.doi.org/10.1128/JVI.01080-07.
24. **Clarke P, Meintzer SM, Moffitt LA, Tyler KL.** 2003. Two distinct phases of virus-induced nuclear factor κB regulation enhance tumor necrosis factor-related apoptosis-inducing ligand-mediated apoptosis in virus-infected cells. J. Biol. Chem. **278:**18092–18100. http://dx.doi.org/10.1074/jbc.M300265200.
25. **Connolly JL, Rodgers SE, Clarke P, Ballard DW, Kerr LD, Tyler KL, Dermody TS.** 2000. Reovirus-induced apoptosis requires activation of transcription factor NF-κB. J. Virol. **74:**2981–2989. http://dx.doi.org/10.1128/JVI.74.7.2981-2989.2000.
26. **Clarke P, Debiasi RL, Meintzer SM, Robinson BA, Tyler KL.** 2005. Inhibition of NF-κB activity and cFLIP expression contribute to viral-induced apoptosis. Apoptosis **10:**513–524. http://dx.doi.org/10.1007/s10495-005-1881-4.
27. **Baty CJ, Sherry B.** 1993. Cytopathogenic effect in cardiac myocytes but not in cardiac fibroblasts is correlated with reovirus-induced acute myocarditis. J. Virol. **67:**6295–6298.
28. **Kobayashi T, Antar AA, Boehme KW, Danthi P, Eby EA, Guglielmi KM, Holm GH, Johnson EM, Maginnis MS, Naik S, Skelton WB, Wetzel JD, Wilson GJ, Chappell JD, Dermody TS.** 2007. A plasmid-based reverse genetics system for animal double-stranded RNA viruses. Cell Host Microbe **1:**147–157. http://dx.doi.org/10.1016/j.chom.2007.03.003.
29. **Zurney J, Kobayashi T, Holm GH, Dermody TS, Sherry B.** 2009. Reovirus μ2 protein inhibits interferon signaling through a novel mechanism involving nuclear accumulation of interferon regulatory factor 9. J. Virol. **83:**2178–2187. http://dx.doi.org/10.1128/JVI.01787-08.
30. **Kobayashi T, Ooms LS, Ikizler M, Chappell JD, Dermody TS.** 2010. An improved reverse genetics system for mammalian orthoreoviruses. Virology **398:**194–200. http://dx.doi.org/10.1016/j.virol.2009.11.037.
31. **Smith RE, Zweerink HJ, Joklik WK.** 1969. Polypeptide components of virions, top component and cores of reovirus type 3. Virology **39:**791–810. http://dx.doi.org/10.1016/0042-6822(69)90017-8.
32. **Holm GH, Zurney J, Tumilasci V, Leveille S, Danthi P, Hiscott J, Sherry B, Dermody TS.** 2007. Retinoic acid-inducible gene-I and interferon-beta promoter stimulator-1 augment proapoptotic responses following mammalian reovirus infection via interferon regulatory factor-3. J. Biol. Chem. **282:**21953–21961. http://dx.doi.org/10.1074/jbc.M702112200.
33. **Sherry B, Baty CJ, Blum MA.** 1996. Reovirus-induced acute myocarditis in mice correlates with viral RNA synthesis rather than generation of infectious virus in cardiac myocytes. J. Virol. **70:**6709–6715.
34. **Stewart MJ, Smoak K, Blum MA, Sherry B.** 2005. Basal and reovirus-induced beta interferon (IFN-β) and IFN-β-stimulated gene expression are cell type specific in the cardiac protective response. J. Virol. **79:**2979–2987. http://dx.doi.org/10.1128/JVI.79.5.2979-2987.2005.
35. **Irvin SC, Zurney J, Ooms LS, Chappell JD, Dermody TS, Sherry B.** 2012. A single-amino-acid polymorphism in reovirus protein μ2 determines repression of interferon signaling and modulates myocarditis. J. Virol. **86:**2302–2311. http://dx.doi.org/10.1128/JVI.06236-11.
36. **Yin P, Keirstead ND, Broering TJ, Arnold MM, Parker JS, Nibert ML, Coombs KM.** 2004. Comparisons of the M1 genome segments and encoded μ2 proteins of different reovirus isolates. Virol. J. **1:**6. http://dx.doi.org/10.1186/1743-422X-1-6.
37. **Ivashkiv LB.** 2009. Cross-regulation of signaling by ITAM-associated receptors. Nat. Immunol. **10:**340–347. http://dx.doi.org/10.1038/ni.1706.
38. **Bradshaw JM.** 2010. The Src, Syk, and Tec family kinases: distinct types of molecular switches. Cell. Signal. **22:**1175–1184. http://dx.doi.org/10.1016/j.cellsig.2010.03.001.
39. **Parker JS, Broering TJ, Kim J, Higgins DE, Nibert ML.** 2002. Reovirus core protein μ2 determines the filamentous morphology of viral inclusion bodies by interacting with and stabilizing microtubules. J. Virol. **76:**4483–4496. http://dx.doi.org/10.1128/JVI.76.9.4483-4496.2002.

40. **Broering TJ, Parker JS, Joyce PL, Kim J, Nibert ML.** 2002. Mammalian reovirus nonstructural protein μNS forms large inclusions and colocalizes with reovirus microtubule-associated protein μ2 in transfected cells. J. Virol. **76:**8285–8297. http://dx.doi.org/10.1128/JVI.76.16.8285-8297.2002.
41. **Fensterl V, Sen GC.** 2009. Interferons and viral infections. Biofactors **35:**14–20. http://dx.doi.org/10.1002/biof.6.
42. **Du Z, Lang SM, Sasseville VG, Lackner AA, Ilyinskii PO, Daniel MD, Jung JU, Desrosiers RC.** 1995. Identification of a *nef* allele that causes lymphocyte activation and acute disease in macaque monkeys. Cell **82:** 665–674. http://dx.doi.org/10.1016/0092-8674(95)90038-1.
43. **Luo W, Peterlin BM.** 1997. Activation of the T-cell receptor signaling pathway by Nef from an aggressive strain of simian immunodeficiency virus. J. Virol. **71:**9531–9537.
44. **Scholle F, Longnecker R, Raab-Traub N.** 1999. Epithelial cell adhesion to extracellular matrix proteins induces tyrosine phosphorylation of the Epstein-Barr virus latent membrane protein 2: a role for C-terminal Src kinase. J. Virol. **73:**4767–4775.
45. **Burkhardt AL, Bolen JB, Kieff E, Longnecker R.** 1992. An Epstein-Barr virus transformation-associated membrane protein interacts with src family tyrosine kinases. J. Virol. **66:**5161–5167.
46. **Wisniewski ML, Werner BG, Hom LG, Anguish LJ, Coffey CM, Parker JS.** 2011. Reovirus infection or ectopic expression of outer capsid protein micro1 induces apoptosis independently of the cellular proapoptotic proteins Bax and Bak. J. Virol. **85:**296–304. http://dx.doi.org/10.1128/JVI.01982-10.
47. **Coffey CM, Sheh A, Kim IS, Chandran K, Nibert ML, Parker JS.** 2006. Reovirus outer capsid protein micro1 induces apoptosis and associates with lipid droplets, endoplasmic reticulum, and mitochondria. J. Virol. **80:**8422–8438. http://dx.doi.org/10.1128/JVI.02601-05.
48. **Danthi P, Coffey CM, Parker JS, Abel TW, Dermody TS.** 2008. Independent regulation of reovirus membrane penetration and apoptosis by the μ1 ϕ domain. PLoS Pathog. **4:**e1000248. http://dx.doi.org/10.1371/journal.ppat.1000248.
49. **Hansberger MW, Campbell JA, Danthi P, Arrate P, Pennington KN, Marcu KB, Ballard DW, Dermody TS.** 2007. IκB kinase subunits alpha and gamma are required for activation of NF-κB and induction of apoptosis by mammalian reovirus. J. Virol. **81:**1360–1371. http://dx.doi.org/10.1128/JVI.01860-06.
50. **Lu J, Lin WH, Chen SY, Longnecker R, Tsai SC, Chen CL, Tsai CH.** 2006. Syk tyrosine kinase mediates Epstein-Barr virus latent membrane protein 2A-induced cell migration in epithelial cells. J. Biol. Chem. **281:** 8806–8814. http://dx.doi.org/10.1074/jbc.M507305200.
51. **Lagunoff M, Lukac DM, Ganem D.** 2001. Immunoreceptor tyrosine-based activation motif-dependent signaling by Kaposi's sarcoma-associated herpesvirus K1 protein: effects on lytic viral replication. J. Virol. **75:**5891–5898. http://dx.doi.org/10.1128/JVI.75.13.5891-5898.2001.
52. **Lee BS, Lee SH, Feng P, Chang H, Cho NH, Jung JU.** 2005. Characterization of the Kaposi's sarcoma-associated herpesvirus K1 signalosome. J. Virol. **79:**12173–12184. http://dx.doi.org/10.1128/JVI.79.19.12173-12184.2005.
53. **Ross SR, Schmidt JW, Katz E, Cappelli L, Hultine S, Gimotty P, Monroe JG.** 2006. An immunoreceptor tyrosine activation motif in the mouse mammary tumor virus envelope protein plays a role in virus-induced mammary tumors. J. Virol. **80:**9000–9008. http://dx.doi.org/10.1128/JVI.00788-06.
54. **Geimonen E, Fernandez I, Gavrilovskaya IN, Mackow ER.** 2003. Tyrosine residues direct the ubiquitination and degradation of the NY-1 hantavirus G1 cytoplasmic tail. J. Virol. **77:**10760–10868. http://dx.doi.org/10.1128/JVI.77.20.10760-10768.2003.
55. **Lagunoff M, Majeti R, Weiss A, Ganem D.** 1999. Deregulated signal transduction by the K1 gene product of Kaposi's sarcoma-associated herpesvirus. Proc. Natl. Acad. Sci. U. S. A. **96:**5704–5709. http://dx.doi.org/10.1073/pnas.96.10.5704.
56. **Miller CL, Arnold MM, Broering TJ, Hastings CE, Nibert ML.** 2010. Localization of mammalian orthoreovirus proteins to cytoplasmic factory-like structures via nonoverlapping regions of μNS. J. Virol. **84:**867–882. http://dx.doi.org/10.1128/JVI.01571-09.
57. **Miller CL, Broering TJ, Parker JS, Arnold MM, Nibert ML.** 2003. Reovirus sigma NS protein localizes to inclusions through an association requiring the μ NS amino terminus. J. Virol. **77:**4566–4576. http://dx.doi.org/10.1128/JVI.77.8.4566-4576.2003.
58. **Faruki S, Geahlen RL, Asai DJ.** 2000. Syk-dependent phosphorylation of microtubules in activated B lymphocytes. J. Cell Sci. **113**(Pt 14)**:**2557–2565.
59. **Iwakiri D, Minamitani T, Samanta M.** 2013. Epstein-Barr virus latent membrane protein 2A contributes to anoikis resistance through ERK activation. J. Virol. **87:**8227–8234. http://dx.doi.org/10.1128/JVI.01089-13.
60. **Fotheringham JA, Coalson NE, Raab-Traub N.** 2012. Epstein-Barr virus latent membrane protein-2A induces ITAM/Syk- and Akt-dependent epithelial migration through αv-integrin membrane translocation. J. Virol. **86:**10308–10320. http://dx.doi.org/10.1128/JVI.00853-12.
61. **Kim HH, Grande SM, Monroe JG, Ross SR.** 2012. Mouse mammary tumor virus suppresses apoptosis of mammary epithelial cells through ITAM-mediated signaling. J. Virol. **86:**13232–13240. http://dx.doi.org/10.1128/JVI.02029-12.
62. **Willems F, Andris F, Xu D, Abramowicz D, Wissing M, Goldman M, Leo O.** 1995. The induction of human T cell unresponsiveness by soluble anti-CD3 MAb requires T cell activation. Int. Immunol. **7:**1593–1598. http://dx.doi.org/10.1093/intimm/7.10.1593.
63. **Breun LA, Broering TJ, McCutcheon AM, Harrison SJ, Luongo CL, Nibert ML.** 2001. Mammalian reovirus L2 gene and lambda2 core spike protein sequences and whole-genome comparisons of reoviruses type 1 Lang, type 2 Jones, and type 3 Dearing. Virology **287:**333–348. http://dx.doi.org/10.1006/viro.2001.1052.
64. **Dermody TS, Schiff LA, Nibert ML, Coombs KM, Fields BN.** 1991. The S2 gene nucleotide sequences of prototype strains of the three reovirus serotypes: characterization of reovirus core protein sigma 2. J. Virol. **65:** 5721–5731.